⌘ *Author's Choice*

Procollagen C-proteinase Enhancer Stimulates Procollagen Processing by Binding to the C-propeptide Region Only*⑤

Sandrine Vadon-Le Goff[‡1], **Daniel Kronenberg**[‡§1,2], **Jean-Marie Bourhis**[‡], **Cécile Bijakowski**[‡], **Nicolas Raynal**[¶3], **Florence Ruggiero**[∥], **Richard W. Farndale**[¶], **Walter Stöcker**[§], **David J. S. Hulmes**[‡4], and **Catherine Moali**[‡]

From the [‡]*Institut de Biologie et Chimie des Protéines, CNRS/Université Lyon 1 FRE3310, 69367 Lyon Cedex 7, France, the* [§]*Institute of Zoology, Department of Cell and Matrix Biology, Johannes Gutenberg University, 55128 Mainz, Germany, the* [¶]*Department of Biochemistry, University of Cambridge, Cambridge CB2 1QW, United Kingdom, and the* [∥]*Institut de Génomique Fonctionnelle de Lyon, ENS de Lyon, UMR CNRS 5242, Université Lyon 1, 69364 Lyon cedex 7, France*

Background: Procollagen C-proteinase enhancer-1 (PCPE-1) is an extracellular glycoprotein that increases activity of certain zinc metalloproteinases involved in tissue development and repair.
Results: PCPE-1 binds uniquely to the C-propeptide region of the procollagen molecule.
Conclusion: PCPE-1 enhances proteolysis by binding solely to the procollagen C-propeptides.
Significance: These data may lead to future applications in the development of antifibrotic therapies.

Bone morphogenetic protein-1 (BMP-1) and the tolloid-like metalloproteinases control several aspects of embryonic development and tissue repair. Unlike other proteinases whose activities are regulated mainly by endogenous inhibitors, regulation of BMP-1/tolloid-like proteinases relies mostly on proteins that stimulate activity. Among these, procollagen C-proteinase enhancers (PCPEs) markedly increase BMP-1/tolloid-like proteinase activity on fibrillar procollagens, in a substrate-specific manner. Here, we performed a detailed quantitative study of the binding of PCPE-1 and of its minimal active fragment (CUB1-CUB2) to three regions of the procollagen III molecule: the triple helix, the C-telopeptide, and the C-propeptide. Contrary to results described elsewhere, we found the PCPE-1-binding sites to be located exclusively in the C-propeptide region. In addition, binding and enhancing activities were found to be independent of the glycosylation state of the C-propeptide. These data exclude previously proposed mechanisms for the action of PCPEs and also suggest new mechanisms to explain how these proteins can stimulate BMP-1/tolloid-like proteinases by up to 20-fold.

Bone morphogenetic protein-1 (BMP-1)[5] and the tolloid-like proteinases have been shown to play crucial roles in both

embryonic development and tissue repair (1–10). These include activation of growth factors, regulation of anti-angiogenic factors, and control of extracellular matrix assembly. In 1996, it was found that BMP-1/tolloid-like proteinases are identical to the previously described procollagen C-proteinases (11, 12), which cleave the C-propeptides from soluble procollagen precursors of the fibrillar collagens, this being the rate-limiting step in the control of fibril assembly (13). As such, BMP-1/tolloid-like proteinases have major implications in connective tissue disorders characterized by excess collagen deposition, notably fibrosis or scarring, which are leading causes of morbidity and mortality worldwide (14–17).

In contrast to other extracellular metalloproteinases such as matrix metalloproteinases (MMPs) whose activities are regulated mainly by endogenous inhibitors such as tissue inhibitors of matrix metalloproteinases (TIMPs), regulation of BMP-1/tolloid-like proteinases (which include BMP-1, mTLD (mammalian tolloid), mTLL-1 (mammalian tolloid-like 1), and mTLL-2) relies mostly on proteins that stimulate activity. These proteins include Tsg (twisted gastrulation) and ONT-1 (olfactomedin-noelin-tarin factor 1), both of which stimulate cleavage of the growth factor antagonist chordin (18, 19). Another example is periostin, which stimulates the proteolytic activation of the cross-linking enzyme lysyl oxidase (20), apparently in concert with fibronectin (21). More extensively studied are, however, the procollagen C-proteinase enhancers (PCPE-1 and PCPE-2), which can stimulate BMP-1/tolloid-like proteinase activity by up to 20-fold (22, 23). Such stimulation is substrate-specific, being limited to C-terminal processing of fibrillar procollagens, with no effect on a variety of other BMP-1/tolloid-like substrates (24, 25). In view of this property, PCPEs are therefore both prototypes for the study of other substrate-specific enhancers and also potential targets for the development of novel antifibrotic therapies (26, 27).

Although much progress has been made (23, 24, 28–32), the mechanism of action of PCPEs remains unclear. The PCPE molecule, which is elongated in shape (29), consists of two CUB (complement/Uegf/BMP-1) domains followed by a NTR

(netrin-like) domain. In solution, PCPE-1 (~50 kDa) behaves as a monomer that binds to the trimeric procollagen molecule (~450 kDa) with nanomolar affinity (28, 30, 31). Interestingly, disruption of the procollagen trimer leads to total loss of enhancing activity (24), suggesting that the binding site is conformational and/or involves more than one chain.

Within the PCPE-1 molecule, the contiguous CUB1-CUB2 region is both necessary and sufficient for enhancing activity, which involves cooperative binding of both domains to the substrate while tethered by a flexible linker (31, 33). Key residues required for enhancing activity have been identified in CUB1 (30). With regard to the procollagen substrate, previous studies suggested that PCPE-1 binds to a region straddling the BMP-1 cleavage site, thereby inducing a conformational change that facilitates proteolytic cleavage (24, 28). This would necessitate binding sites for PCPE-1 both in the C-propeptide region (~90 kDa) and in the C-telopeptide region (the short ~25-residue non-triple-helical region that remains at the C terminus of the collagen molecule following C-propeptide cleavage) (see Fig. 1*A*). In contrast, others have reported that PCPE-1 binds to multiple sites throughout the ~300-nm-long triple-helical region of the procollagen molecule (23).

Given the apparent conflict between the data and the different aspects that remain unexplained, it seemed important to determine precisely where PCPE-1 binds on the large procollagen molecule. In this study, we have used new tools, both proteins and peptides, to compare the binding strength of PCPE-1 on three major regions of the procollagen III molecule: the triple helix, the C-telopeptide, and the C-propeptide. We found the binding sites to be located exclusively in the C-propeptide region. In addition, both binding and enhancing activities were shown to be independent of the glycosylation state of the C-propeptide. These data help better map the binding sites of PCPE-1 on fibrillar procollagens and also exclude previously proposed mechanisms for PCPE action.

EXPERIMENTAL PROCEDURES

Materials—Acid-soluble collagen I (from rat tail tendon, with intact telopeptides) and pepsin-extracted collagen III (from human placenta, without telopeptides) were from BD Biosciences. Triple-helical peptide toolkits based on human collagen II and III were synthesized and characterized as described (34, 35). Only peptide C-telo was newly synthesized for the purposes of this study.

Molecular Biology—All mutations and deletions were generated with the QuikChange XL site-directed mutagenesis kit from Stratagene. The coding sequence for mini-procollagen III in pCEP4 (24) was used as a template to generate mutants E150A, K151A, and N306Q (see Fig. 1*B*) as well as the C-propeptide trimer of human procollagen III (CPIII) in 293-EBNA cells. The first three mutants were obtained using overlapping primers with mutated bases in the middle and melting temperatures above 72 °C. For the C-propeptide, a forward primer matching the DNA sequence of the C-propeptide and a reverse primer corresponding to the signal peptide of procollagen III were used to delete the c-Myc tag, the triple-helical region, and the C-telopeptide. In the latter case, phosphorylated primers were used, and the PCR product was ligated before transforma-

tion in XL1-Blue bacterial cells. CPIII-His was amplified by PCR from the N306Q mini-procollagen III + pCEP4 construct. The resulting fragment was inserted into the pBAC3 vector (Novagen) in-frame with an N-terminal His_6 tag. Recombinant baculovirus was obtained using the BacMagic-2 kit (Novagen) according to the manufacturer's protocol.

Protein Production, Purification, and Characterization—All recombinant proteins are human forms. Mini-procollagen III, PCPE-1, PCPE-1-His, and BMP-1-FLAG (referred to as BMP-1 below) were produced in 293-EBNA cells as described (24, 30). CUB1-CUB2 was produced by limited proteolysis of full-length PCPE-1 (31). Mini-procollagen III mutants E150A, K151A, and N306Q were produced and purified as described for the parent molecule, including an anti-PCPE column to remove endogenous PCPE (24). For production of CPIII in 293-EBNA cells, conditioned medium was purified as described for the protein expressed in insect cells (36), with a final gel filtration step on a Superdex 200 HR 16/60 prep-grade column (GE Healthcare) in 20 mM HEPES (pH 7.4) and 0.15 M NaCl. For expression of CPIII-His, *Trichoplusia ni* insect cells (High Five™ BTI-TN-5B1-4, Invitrogen) were cultured in spinner flasks with Express Five medium (Invitrogen) supplemented with L-glutamine and penicillin/streptomycin. Infection with recombinant baculovirus was performed using a multiplicity of infection of 1 when the cell density reached 1×10^6 cells/ml. After 3 days of infection, the culture medium was collected, and the pH was adjusted to 6.5. The medium was then loaded onto an IMAC column (GE Healthcare) precharged with Co^{2+} and eluted with 50 mM Tris (pH 8), 0.3 M NaCl, 5 mM $CaCl_2$, and 0.25 M imidazole. A second purification step was performed on a Superdex 200 HR 16/60 prep-grade column as described for CPIII. N-terminal sequencing by Edman degradation and mass spectrometry were performed at the protein microanalysis facility of UMS 3444 (Lyon, France).

For co-immunoprecipitation, 500 nM mini-procollagen III was first cleaved in 50 mM Tris (pH 7.4), 0.15 M NaCl, 5 mM $CaCl_2$, and 0.02% Brij-35 for 3 h at 37 °C in the presence of 30 nM BMP-1 and 500 nM PCPE-1-His (volume of 200 μl). 50 μl of anti-PCPE-Sepharose was then added for 3 h at room temperature. Control experiments with 500 nM mini-procollagen III alone and a mixture of mini-procollagen III and PCPE-1-His (both at 500 nM) were also performed. Suspensions were loaded onto 500-μl Handee spin columns (Pierce). After five washing steps by pulse centrifugation with 100 μl of 50 mM Tris (pH 7.4), 0.15 M NaCl, and 1% Triton X-100, proteins were eluted with 100 mM glycine HCl (pH 2.5) and analyzed by SDS-PAGE (15% acrylamide, reducing conditions) and Western blotting. Intact mini-procollagen III and its N-terminal fragment were detected with anti-c-Myc antibody, whereas the C-propeptide was detected with a monoclonal antibody directed against the N-terminal region of CPIII (48D34) (37).

ELISA—Peptides were dissolved at 1 mg/ml in 0.01 M acetic acid and diluted to 10 μg/ml in 10 mM Tris-HCl (pH 7.4) and 0.15 M NaCl. 96-Well Immulon 4HBX microtiter plates (Thermo Scientific) were coated overnight at 4 °C with 100 μl of 10 μg/ml peptide or protein. The rest of the protocol was as described previously (31) using PCPE-1-His at a concentration of 2 μg/ml for 2 h at room temperature.
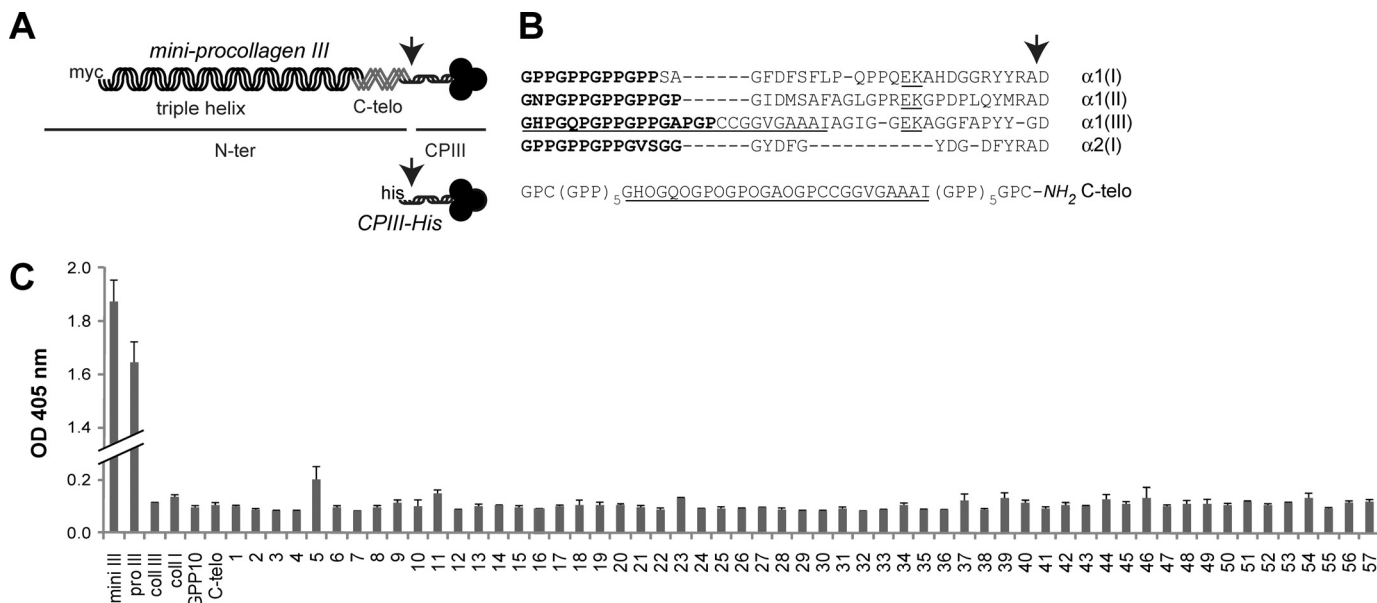
FIGURE 1. *A*, diagrammatic representations of CPIII-His and mini-procollagen III. The triple-helical region is represented by *wavy lines*, the C-telopeptide by *zigzag lines*, and the putative coiled coil by the *stalk* in the C-propeptide trimer. *Arrows* indicate the BMP-1 cleavage site. *B*, alignment of C-telopeptides from the α_1-chains of collagens I–III and the α_2-chain of collagen I (note that collagens II and III are homotrimers consisting of three identical α_1-chains, whereas collagen I is a heterotrimer consisting of two α_1-chains and one α_2-chain). The end of the triple-helical region is in *boldface* (note that prolines in the *Y* position of the G*XY* triplet are normally hydroxylated), and the conserved EK sequence is *underlined*. Also *underlined* is the sequence from collagen III used to make C-telo, shown in full below (where *O* represents hydroxyproline). *C*, representative set of ELISA experiments performed in triplicate showing PCPE-1-His interactions with coated mini-procollagen III (*mini III*), procollagen III (*pro III*), human collagen III (*coll III*), rat collagen I (*coll I*), (Gly-Pro-Pro)$_{10}$, C-telo, and triple-helical peptides from the collagen III toolkit (35). The plot shows binding of PCPE-1-His detected as described previously (31).

Activity Assays—PCPE enhancing activity was analyzed as described (31, 38) using reaction volumes of 20–50 μl with incubation times and protein concentrations as indicated.

Surface Plasmon Resonance—These experiments were performed with a Biacore T100 system (GE Healthcare) at the Protein Production and Analysis Facility of UMS 3444. Immobilization of ligands (mini-procollagen III and mutants, C-propeptide III and variants, and PCPE-1-His), regeneration of sensor chips, and analysis of kinetics were as described previously (30, 31). Sensorgrams were recorded at 25 °C with 10 mM HEPES (pH 7.4), 0.15 M NaCl, 5 mM CaCl$_2$, and 0.05% surfactant P20 as running buffer.

RESULTS

Role of the Collagen Triple-helical Region—On the basis of evidence that PCPEs co-centrifuged with collagens when fibrils were reconstituted *in vitro* and rotary shadowing data, Steiglitz *et al.* (23) concluded that these proteins were capable of binding to the collagen triple helix. In contrast, PCPE-1 appears to have no effect on the kinetics of collagen I fibril reconstitution *in vitro* (32). To investigate this question further, we set up an ELISA using immobilized collagen I, collagen III, full-length procollagen III, and mini-procollagen III (which lacks the N-propeptide, the N-telopeptide, and all but the 33 most C-terminal Gly-*X*-Y triplets in the triple-helical region) (24). As shown in Fig. 1*C*, no significant interaction of PCPE-1 with collagens I and III could be detected, whereas, as expected, clear signals were obtained with procollagen III or mini-procollagen III, both of which include the C-propeptide region.

To confirm these results and to assess the possibility of cryptic sites, we also tested possible PCPE-1 binding to sets of overlapping triple-helical peptides (each representing nine successive Gly-*X*-Y motifs) based on the entire triple-helical regions of human collagens II and III (34, 35). As also shown in Fig. 1*C*, none of the 57 collagen III peptides gave a signal that was significantly higher than that of the (Gly-Pro-Pro)$_{10}$ control peptide. Similar results were obtained with the triple-helical peptides from collagen II (data not shown). These data also support the absence of interaction between PCPE-1 and the collagen triple helix.

Role of the C-telopeptide Region—The C-telopeptide region of the collagen molecule is known to play important roles in the assembly and cross-linking of collagen fibrils (39). We previously identified a number of common features within the C-telopeptide regions of the major fibrillar collagens that might be involved in PCPE-1 binding (24). These include (Fig. 1*B*), within the α_1-chains, (i) a mostly hydrophobic 5–10-residue motif, (ii) two strictly conserved and contiguous residues (EK) at the site of cross-linking initiation by lysyl oxidases, and (iii) a Y(Y/M)(R/-) motif preceding the P1 residue of the BMP-1 cleavage site.

To probe the role of the hydrophobic motif, we synthesized a trimeric peptide covering the end of the triple helix and most of the hydrophobic sequence found in collagen III (C-telo; see Fig. 1*B* for the sequence). By ELISA, this peptide also failed to interact with PCPE-1 (Fig. 1*C*). This was confirmed by surface plasmon resonance and by the lack of effect of the peptide on PCPE enhancing activity at concentrations up to 1 μM (supplemental Fig. 1*A*). Therefore, this motif does not seem to be involved in PCPE binding.

To investigate the possible role of the conserved EK sequence, these residues (Glu-150 and Lys-151 in mini-procollagen III) were individually mutated to alanines. When assayed
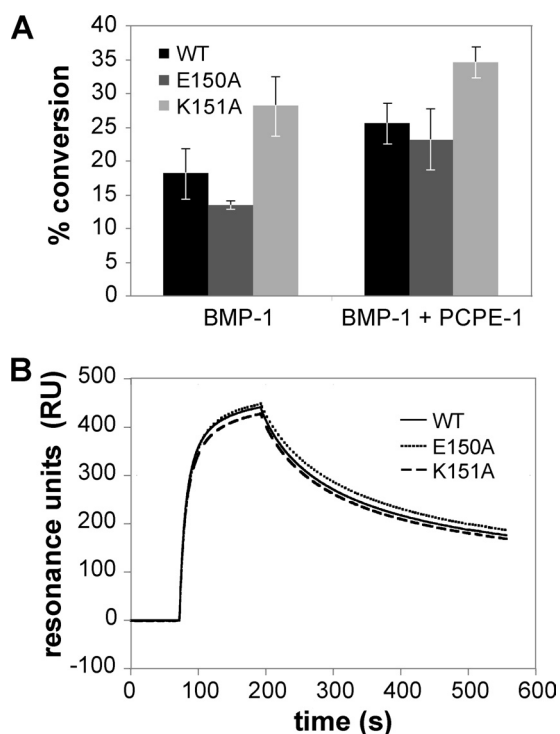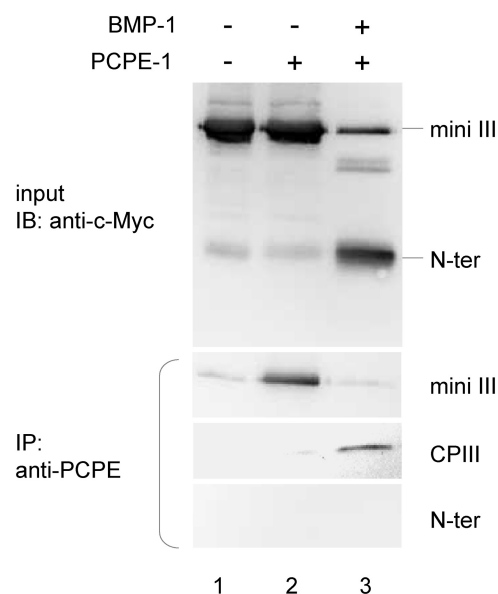
FIGURE 2. **Effects of mutations E150A and K151A in mini-procollagen III on BMP-1 activity (*A*) and PCPE-1 binding (*B*).** For activity assays (*A*), WT or mutant mini-procollagen III (342 nM) was incubated either with BMP-1 alone or with BMP-1 and PCPE (342 nM), with BMP-1 concentrations and incubation times (16 nM for 1 h or 3.8 nM for 25 min, respectively) adjusted to give ~30% conversion (*i.e.* within the linear range). Percentage conversion to CPIII was determined by SDS-PAGE and quantitation after SYPRO Ruby staining. *Error bars* show S.D. (*n* = 6). For Biacore studies (*B*), mini-procollagen III or mutants (all at 128 nM) were injected over immobilized PCPE-1-His (514 resonance units) at 50 μl/min.

FIGURE 3. **Co-immunoprecipitation of PCPE-1 and the C-propeptide region of mini-procollagen III.** Mini-procollagen III was first preincubated alone (*lane 1*) or in the presence of PCPE-1-His (*lane 2*) or PCPE-1-His and BMP-1 (*lane 3*) and then immunoprecipitated with anti-PCPE-Sepharose. Mini-procollagen III (*mini III*) and the released N-terminal fragment (*N-ter*) were detected with anti-c-Myc monoclonal antibody 9E10, whereas CPIII was detected with anti-CPIII monoclonal antibody 48D34. *IB*, immunoblot.

for BMP-1 cleavage in the absence of PCPE-1 (Fig. 2*A*), activity was slightly increased by the K151A mutation but was unchanged by the E150A mutation. Corresponding variations were seen in the presence of PCPE-1, suggesting a direct effect of the mutation on enzyme-substrate recognition rather than on enhancement. To measure interactions with PCPE-1 directly, we used surface plasmon resonance (Fig. 2*B*). When equal amounts of mini-procollagen III and of its E150A and K151A mutants were injected over immobilized PCPE, the curves obtained were strikingly similar in terms of maximal response and shape. As a consequence, these residues do not seem to be involved in the interaction with PCPE-1.

A further indication that the C-telopeptides were not involved in binding to PCPE-1 was obtained by co-immunoprecipitation. For this experiment, mini-procollagen III was incubated with PCPE-1 in the absence or presence of BMP-1. In the latter case, a mixture of CPIII and the N-terminal fragment of mini-procollagen III (Fig. 1*A*, *N-ter*) was produced. PCPE-1 was found to coprecipitate with mini-procollagen III and CPIII (Fig. 3) but not with the N-terminal fragment, which encompasses the C-telopeptide region.

These data strongly support the idea that PCPE-1 does not interact with the C-telopeptide region following procollagen cleavage by BMP-1. Weak binding to the C-telopeptides in the intact procollagen molecule cannot be totally excluded, however, because cleavage might either disrupt cooperative binding

involving multiple sites (either side of the cleavage site, for example) and/or lead to a conformational change in the C-telopeptide, thereby releasing PCPE-1. This point is addressed below.

Role of the C-propeptide Region—Previous surface plasmon resonance studies (28) suggested that PCPE-1 has a much greater affinity for procollagen than for the isolated C-propeptide trimer, suggesting that PCPE-1 binding might straddle the BMP-1 cleavage site and thereby induce a conformational change in the substrate. In view of the results presented above, however, we decided to reinvestigate this question in some detail. We immobilized CPIII and mini-procollagen III or variants thereof and injected PCPE-1 or its minimal active fragment (CUB1-CUB2) (31) in the mobile phase.

For immobilized mini-procollagen III (31), the data were best described using a "heterogeneous ligand" model involving two binding sites on the immobilized partner, both contributing approximately equally to the signal. The lowest equilibrium dissociation constant (K_D) was ~0.4 nM and the highest was ~8 nM for both PCPE-1 and CUB1-CUB2 (Table 1; see also supplemental Table 1 for kinetic constants). Similar results were obtained when PCPE-1 was immobilized (supplemental Fig. 1*B*). For immobilized CPIII, the data were also best described using the heterogeneous ligand model, albeit that the contribution of the lowest K_D was relatively small (Table 1). Although there were some differences between the K_D values when comparing mini-procollagen III and CPIII (no more than an order of magnitude), these were much less than those previously reported using full-length procollagen (28). This can be explained by the use of alternative approaches for the surface plasmon resonance studies, thereby overcoming the problems usually associated with the use of large matrix molecules (aggregation, nonspecific binding, and mass transport effects),

TABLE 1

Surface plasmon resonance data for the interactions of PCPE-1 and CUB1-CUB2 with immobilized CPIII, CPIII-His, mini-procollagen III, and the N306Q mutant of mini-procollagen III

PCPE and CUB1-CUB2 (0.39–50 nM) were injected over 500–900 resonance units of immobilized proteins. Means are shown of at least three independent experiments (with different surfaces), with errors calculated from the standard deviations in the kinetic constants k_a and k_d (supplemental Table 1). In all cases, the best fits were obtained with the heterogeneous ligand model. Complete sets of kinetic data are given in supplemental Table 1. Data for mini-procollagen III are taken from Kronenberg *et al.* (31).

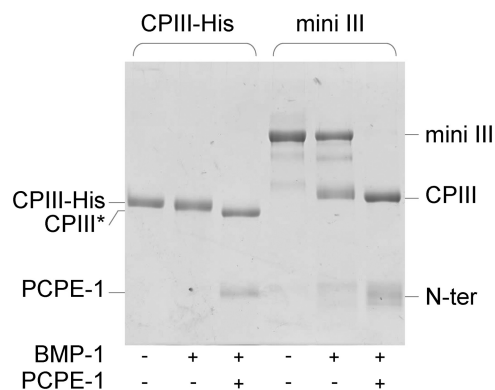|	PCPE-1				
	$K_{D(1)}$	$K_{D(2)}$	$R_{max(1)}$	$R_{max(2)}$	χ^2
	*n*M	*n*M	%	%	
CPIII	4.7 ± 0.8	17 ± 2	8 ± 1	92 ± 1	0.54–0.69
CPIII-His	5.9 ± 0.9	15 ± 2	17 ± 2	83 ± 2	0.44–0.46
Mini-procollagen III	0.31 ± 0.10	6.8 ± 2.7	47 ± 10	53 ± 10	1.4–3.6
Mini-procollagen III N306Q	0.66 ± 0.38	10 ± 3.5	46 ± 11	54 ± 11	0.95–4.6

	CUB1-CUB2				
	$K_{D(1)}$	$K_{D(2)}$	$R_{max(1)}$	$R_{max(2)}$	χ^2
	*n*M	*n*M	%	%	
CPIII	4.6 ± 2.6	28 ± 10	19 ± 4	81 ± 4	0.08–0.39
CPIII-His	12.8 ± 7.5	27 ± 11	22 ± 5	78 ± 5	0.10–0.96
Mini-procollagen III	0.51 ± 0.16	8.4 ± 3.7	61 ± 10	39 ± 10	0.59–1.81
Mini-procollagen III N306Q	0.74 ± 0.11	12.6 ± 1.2	51 ± 1	49 ± 1	0.61–0.89

in which shortened forms of the substrate were immobilized, and the smaller binding partner (PCPE-1 or CUB1-CUB2) was used as an analyte. Calcium ions were also present, in contrast to previous studies (28), to match more closely the conditions used for the activity assays. In this way, we achieved a satisfactory fit to the surface plasmon resonance data in all cases, and there were only small differences in the affinities of PCPE-1 (or CUB1-CUB2) for the different forms of mini-procollagen III and CPIII. We conclude that the affinities of PCPE-1 and CUB1-CUB2 for mini-procollagen III and CPIII are similar, which reinforces the idea that binding is to the C-propeptide only.

If PCPE-1 depends only on the C-propeptide region for binding to the procollagen molecule and enhancing its cleavage by BMP-1, we reasoned that it should continue to function even when the entire sequence of procollagen III located N-terminal to the BMP-1 cleavage site is replaced. To check this, we made a new potential substrate called CPIII-His (Fig. 1*A*), composed of an N-terminal His tag, followed by a Ser-Ala sequence (Ala is often found at P1 in BMP-1 substrates) and then the entire C-propeptide (mutated at the *N*-glycosylation site; see below) beginning at the usual Asp residue (Asp-1222, numbered from the start of the signal sequence). This substrate could still be cleaved by BMP-1, and strikingly, PCPE-1 continued to show enhancing activity (Fig. 4). By N-terminal sequencing, after cleavage in the presence of PCPE-1, we found the cleavage site to be identical to that of CPIII derived from procollagen III (beginning Asp-Glu-Pro-Met-Asp). This experiment clearly demonstrates that the C-telopeptide of procollagen III is not required for enhancement by PCPE-1.

Finally, we investigated the role of glycosylation in the C-propeptide region in PCPE-1 enhancing activity. (Each chain contains a single *N*-linked glycosylation site at residue 142 in the procollagen III C-propeptide, numbered from the P1′ aspartate in the BMP-1 cleavage site.) As determined by surface plasmon resonance (Fig. 5*A*), binding of PCPE-1 to immobilized (nonglycosylated) CPIII-His was associated with K_D values (heterogeneous ligand model) that were indistinguishable from those for (glycosylated) CPIII (Table 1). Similarly, binding constants were unchanged by mutation of the *N*-glycosylation site

FIGURE 4. **Cleavage of CPIII-His by BMP-1 in the presence and absence of PCPE-1-His.** CPIII-His (450 nM) was incubated alone, with BMP-1 (19 nM), or with BMP-1 (19 nM) and PCPE-1-His (450 nM) for 2 h. For comparison, mini-procollagen III (*mini III*) was incubated under the same conditions. Note that CPIII* (the product of CPIII-His cleavage by BMP-1) differs in size from CPIII (from mini-procollagen III) by the absence of *N*-glycosylation in the former. In the absence of PCPE-1, cleavage of CPIII-His by BMP-1 is relatively inefficient. *N-ter*, N-terminal fragment.

(N306Q, numbered from the start of mini-procollagen III) in the C-propeptide region of mini-procollagen III (Fig. 5*B* and Table 1), as was cleavage by BMP-1, with or without PCPE-1 (Fig. 5*B*, *inset*). We conclude that *N*-glycosylation of the C-propeptide is not involved in PCPE-1 binding or enhancing activity.

Taken together, these data indicate that PCPE-1 binds exclusively to the C-propeptide region of procollagen III in a glycosylation-independent manner and that this is sufficient to trigger enhancement of the catalytic activity of BMP-1.

DISCUSSION

Here, we have identified the site of interaction of PCPE-1 on fibrillar procollagens, thus providing new insights into the mechanism by which this substrate-specific enhancer can turn a rather slow enzymatic process into a much more efficient and selective biosynthetic machinery. To our surprise, the conclusions that derive from this study are somewhat in contradiction with previous hypotheses.

One hypothesis suggests that PCPEs compete with BMP-1/tolloid-like proteinases for binding to the triple-helical region
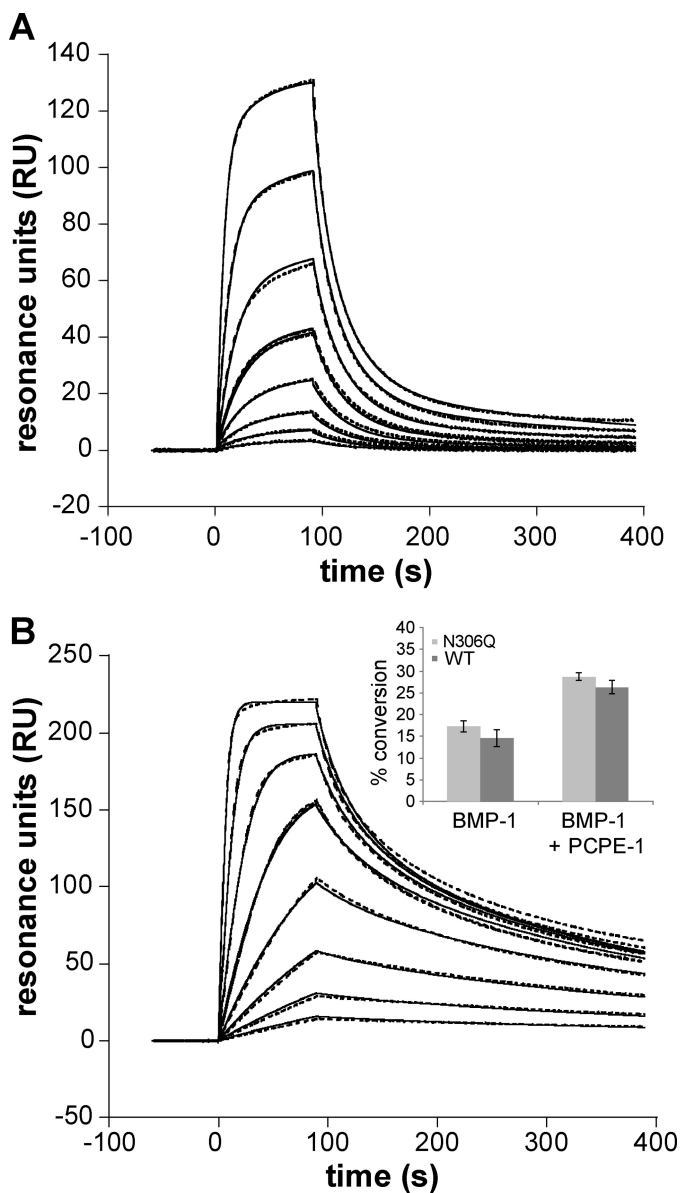
FIGURE 5. Surface plasmon resonance analysis of the interactions of PCPE-1 with immobilized CPIII-His (700 resonance units; *A*) and immobilized mini-procollagen III mutant N306Q (800 resonance units; *B*). In both cases, increasing concentrations of PCPE-1 (0.39–50 nM, 6.25 nM concentration injected twice) were injected at 30 μl/min. Best fits are also shown (*full lines*; heterogeneous ligand model). See Table 1 and supplemental Table 1 for kinetic and equilibrium constants. The *inset* in *B* shows that the *N*-glycosylation of mini-procollagen III at Asn-306 is not important for cleavage by BMP-1 in the presence and absence of PCPE-1-His. The same incubation conditions as described in the legend to Fig. 2*A* were used, with BMP-1 concentrations adjusted to give 15–30% conversion. Quantitation was by SDS-PAGE and SYPRO Ruby staining. *Error bars* show S.D. (*n* = 4).

(23). In this model, the latter acts as a local reservoir for the proteinase, which is released by PCPE binding. This model is not consistent, however, with the data presented here, which show that strong binding of PCPE is exclusively to the C-propeptide region. In a second model, the interaction of PCPE with the C-terminal region of the procollagen molecule is thought to trigger a conformational change in the substrate that facilitates proteolytic cleavage (22, 28). Although, in general, this concept remains a possibility, the idea that PCPE-1 straddles both sides (*i.e.* both N- and C-terminal) of the BMP-1 cleavage site (28) is

made obsolete by the results reported here. Exclusive binding of PCPE-1 to the C-propeptide region was supported by the lack of interaction with the C-telopeptide region, as shown by the ELISA and Biacore assays, by the coprecipitation data, and by the ability of PCPE-1 to enhance BMP-1 activity using CPIII-His, which is devoid of the C-telopeptide.

It has been shown previously by cross-linking experiments and activity assays that the stoichiometry of the PCPE-1·CPIII complex is 1:1 (28, 40). This is despite the trimeric nature of CPIII, which might otherwise suggest a 3:1 stoichiometry. These data, coupled with the observation that PCPE-1 does not enhance BMP-1 cleavage of procollagen III after heat denaturation and reduction (24), suggest that the binding site for PCPE-1 involves multiple polypeptide chains. The low resolution structure of CPIII as determined by small angle x-ray scattering shows a trilobed structure emerging from a common stalk (36). This stalk is thought to correspond to the junction region in which the three polypeptide chains are intimately intertwined. It therefore seems reasonable to think that PCPE-1 actually binds to this region, close to the BMP-1 cleavage site.

The observation that PCPE-1 binds exclusively to the C-propeptide region of the procollagen molecule and remains bound after cleavage by BMP-1 puts a new perspective on the possible mechanism of action of this enhancer protein. Formation of the PCPE-1·C-propeptide complex, close to the BMP-1 cleavage site, must somehow modify the presentation of the substrate to the enzyme, leading to the observed increase in k_{cat}/K_m seen in the presence of PCPE-1 (22). This could occur by increasing the affinity of the enzyme for the substrate (lowering K_m) and/or increasing the catalytic activity (increasing k_{cat}). Such changes might be linked to the creation of additional anchorage points for the enzyme, compared with substrate alone, and/or to conformational changes in the substrate, in the enzyme, or in both. For example, in the case of matrix metalloproteinases, binding of the linker/hemopexin or fibronectin II-like regions to the substrate can lead to local unwinding, thereby accelerating cleavage of triple-helical collagens (41, 42). By analogy, PCPEs might interact with the trimeric procollagen substrate and present individual chains for cleavage by BMP-1/tolloid-like proteinases. Another possibility is that interaction with the PCPE·substrate complex induces a change in the conformation of the enzyme. Recent observations on the low resolution structures of BMP-1, mTLD, and mTLL-1 show that the non-catalytic CUB and EGF domains can partially occlude the active site (43, 44). Interaction with the PCPE·substrate complex might therefore expose the catalytic domain, thereby accelerating proteolysis. In this regard, there is evidence that the CUB2-EGF-CUB3 region of BMP-1 is involved in PCPE activity (25). Structural studies are clearly required to elucidate the mechanism of action of PCPEs further.

Identification of the site of interaction of PCPE-1 with the procollagen substrate could have important implications for the development of novel strategies to prevent the excessive accumulation of collagen seen in fibrotic diseases. In view of the substrate-specific nature of PCPE enhancing activity, which appears to be limited to C-terminal processing of the major fibrillar procollagens (24), strategies aimed at blocking the action of PCPEs would seem to be promising, especially as there

is evidence of PCPE up-regulation in liver and cardiac fibrosis (26, 27) and in corneal scarring.[6]

In summary, this study gives new insights into how PCPEs bind to procollagen molecules and enhance the action of BMP-1/tolloid-like proteinases. The C-propeptide region definitely appears to be the main target for PCPE action. Now that the interaction sites have been located at the scale of domains both in PCPEs (30, 31) and in procollagen, future work will focus on structural aspects of this interaction, which leads to such a spectacular increase in the catalytic efficiency.

REFERENCES

1. Suzuki, A., Shioda, N., and Ueno, N. (1995) *Dev. Growth Differ.* **37,** 581–588
2. Marqués, G., Musacchio, M., Shimell, M. J., Wünnenberg-Stapleton, K., Cho, K. W., and O'Connor, M. B. (1997) *Cell* **91,** 417–426
3. Piccolo, S., Agius, E., Lu, B., Goodman, S., Dale, L., and De Robertis, E. M. (1997) *Cell* **91,** 407–416
4. Clark, T. G., Conway, S. J., Scott, I. C., Labosky, P. A., Winnier, G., Bundy, J., Hogan, B. L., and Greenspan, D. S. (1999) *Development* **126,** 2631–2642
5. Gonzalez, E. M., Reed, C. C., Bix, G., Fu, J., Zhang, Y., Gopalakrishnan, B., Greenspan, D. S., and Iozzo, R. V. (2005) *J. Biol. Chem.* **280,** 7080–7087
6. Ge, G., and Greenspan, D. S. (2006) *J. Cell Biol.* **175,** 111–120
7. Ge, G., Fernández, C. A., Moses, M. A., and Greenspan, D. S. (2007) *Proc. Natl. Acad. Sci. U.S.A.* **104,** 10010–10015
8. Hopkins, D. R., Keles, S., and Greenspan, D. S. (2007) *Matrix Biol.* **26,** 508–523
9. De Robertis, E. M. (2009) *Mech. Dev.* **126,** 925–941
10. Moali, C., and Hulmes, D. J. (2009) *Eur. J Dermatol.* **19,** 552–564
11. Kessler, E., Takahara, K., Biniaminov, L., Brusel, M., and Greenspan, D. S. (1996) *Science* **271,** 360–362
12. Li, S. W., Sieron, A. L., Fertala, A., Hojima, Y., Arnold, W. V., and Prockop, D. J. (1996) *Proc. Natl. Acad. Sci. U.S.A.* **93,** 5127–5130
13. Canty, E. G., and Kadler, K. E. (2005) *J. Cell Sci.* **118,** 1341–1353
14. Turtle, E. D., and Ho, W. B. (2004) *Expert Opin. Ther. Patents* **14,** 1185–1197
15. Wynn, T. A. (2007) *J. Clin. Invest.* **117,** 524–529
16. Bailey, S., Fish, P. V., Billotte, S., Bordner, J., Greiling, D., James, K., McElroy, A., Mills, J. E., Reed, C., and Webster, R. (2008) *Bioorg. Med. Chem. Lett.* **18,** 6562–6567
17. Kobayashi, K., Luo, M., Zhang, Y., Wilkes, D. C., Ge, G., Grieskamp, T., Yamada, C., Liu, T. C., Huang, G., Basson, C. T., Kispert, A., Greenspan, D. S., and Sato, T. N. (2009) *Nat. Cell Biol.* **11,** 46–55
18. Scott, I. C., Blitz, I. L., Pappano, W. N., Maas, S. A., Cho, K. W., and Greenspan, D. S. (2001) *Nature* **410,** 475–478
19. Inomata, H., Haraguchi, T., and Sasai, Y. (2008) *Cell* **134,** 854–865
20. Maruhashi, T., Kii, I., Saito, M., and Kudo, A. (2010) *J. Biol. Chem.* **285,** 13294–13303
21. Huang, G., Zhang, Y., Kim, B., Ge, G., Annis, D. S., Mosher, D. F., and Greenspan, D. S. (2009) *J. Biol. Chem.* **284,** 25879–25888
22. Adar, R., Kessler, E., and Goldberg, B. (1986) *Collagen Relat. Res.* **6,** 267–277
23. Steiglitz, B. M., Keene, D. R., and Greenspan, D. S. (2002) *J. Biol. Chem.* **277,** 49820–49830
24. Moali, C., Font, B., Ruggiero, F., Eichenberger, D., Rousselle, P., François, V., Oldberg, A., Bruckner-Tuderman, L., and Hulmes, D. J. (2005) *J. Biol. Chem.* **280,** 24188–24194
25. Petropoulou, V., Garrigue-Antar, L., and Kadler, K. E. (2005) *J. Biol. Chem.* **280,** 22616–22623
26. Ogata, I., Auster, A. S., Matsui, A., Greenwel, P., Geerts, A., D'Amico, T., Fujiwara, K., Kessler, E., and Rojkind, M. (1997) *Hepatology* **26,** 611–617
27. Kessler-Icekson, G., Schlesinger, H., Freimann, S., and Kessler, E. (2006) *Int. J. Biochem. Cell Biol.* **38,** 358–365
28. Ricard-Blum, S., Bernocco, S., Font, B., Moali, C., Eichenberger, D., Farjanel, J., Burchardt, E. R., van der Rest, M., Kessler, E., and Hulmes, D. J. (2002) *J. Biol. Chem.* **277,** 33864–33869
29. Bernocco, S., Steiglitz, B. M., Svergun, D. I., Petoukhov, M. V., Ruggiero, F., Ricard-Blum, S., Ebel, C., Geourjon, C., Deleage, G., Font, B., Eichenberger, D., Greenspan, D. S., and Hulmes, D. J. (2003) *J. Biol. Chem.* **278,** 7199–7205
30. Blanc, G., Font, B., Eichenberger, D., Moreau, C., Ricard-Blum, S., Hulmes, D. J., and Moali, C. (2007) *J. Biol. Chem.* **282,** 16924–16933
31. Kronenberg, D., Vadon-Le Goff, S., Bourhis, J. M., Font, B., Eichenberger, D., Hulmes, D. J., and Moali, C. (2009) *J. Biol. Chem.* **284,** 33437–33446
32. Steiglitz, B. M., Kreider, J. M., Frankenburg, E. P., Pappano, W. N., Hoffman, G. G., Meganck, J. A., Liang, X., Höök, M., Birk, D. E., Goldstein, S. A., and Greenspan, D. S. (2006) *Mol. Cell. Biol.* **26,** 238–249
33. Hulmes, D. J., Mould, A. P., and Kessler, E. (1997) *Matrix Biol.* **16,** 41–45
34. Konitsiotis, A. D., Raynal, N., Bihan, D., Hohenester, E., Farndale, R. W., and Leitinger, B. (2008) *J. Biol. Chem.* **283,** 6861–6868
35. Raynal, N., Hamaia, S. W., Siljander, P. R., Maddox, B., Peachey, A. R., Fernandez, R., Foley, L. J., Slatter, D. A., Jarvis, G. E., and Farndale, R. W. (2006) *J. Biol. Chem.* **281,** 3821–3831
36. Bernocco, S., Finet, S., Ebel, C., Eichenberger, D., Mazzorana, M., Farjanel, J., and Hulmes, D. J. (2001) *J. Biol. Chem.* **276,** 48930–48936
37. Burchardt, E. R., Heke, M., Kauschke, S. G., Harjes, P., Kohlmeyer, J., Kroll, W., Schauer, M., Schroeder, W., and Voelker, M. (1998) *Matrix Biol.* **17,** 673–677
38. Bekhouche, M., Kronenberg, D., Vadon-Le Goff, S., Bijakowski, C., Lim, N. H., Font, B., Kessler, E., Colige, A., Nagase, H., Murphy, G., Hulmes, D. J., and Moali, C. (2010) *J. Biol. Chem.* **285,** 15950–15959
39. Hulmes, D. J. S. (2008) in *Collagen: Structure and Mechanics* (Fratzl, P., ed) pp. 15–47, Springer, New York
40. Moschcovich, L., Bernocco, S., Font, B., Rivkin, H., Eichenberger, D., Chejanovsky, N., Hulmes, D. J., and Kessler, E. (2001) *Eur. J. Biochem.* **268,** 2991–2996
41. Chung, L., Dinakarpandian, D., Yoshida, N., Lauer-Fields, J. L., Fields, G. B., Visse, R., and Nagase, H. (2004) *EMBO J.* **23,** 3020–3030
42. Tam, E. M., Moore, T. R., Butler, G. S., and Overall, C. M. (2004) *J. Biol. Chem.* **279,** 43336–43344
43. Berry, R., Jowitt, T. A., Ferrand, J., Roessle, M., Grossmann, J. G., Canty-Laird, E. G., Kammerer, R. A., Kadler, K. E., and Baldock, C. (2009) *Proc. Natl. Acad. Sci. U.S.A.* **106,** 8561–8566
44. Berry, R., Jowitt, T. A., Garrigue-Antar, L., Kadler, K. E., and Baldock, C. (2010) *FEBS Lett.* **584,** 657–661